# THE MEASURED PERFORMANCE AND MODEL BASED PERFORMANCE ANALYSIS OF A 16 kW ABSORPTION CHILLER

*Hongxi Yin, Research Associate,*
*David H. Archer, Adjunct Professor of Engineering,*
*Center for Building Performance and Diagnostics,*
*Carnegie Mellon University, Pittsburgh, PA 15213*

**Abstract:** A 16 kW steam driven double-effect water LiBr absorption chiller with parallel solution configuration has been designed, manufactured, and installed for the Intelligent Workplace at Carnegie Mellon University. This particular chiller is driven by saturated steam at a pressure of 6 bar and is based on a 55% (by mass) LiBr/water solution. A steady-state computational model for the chiller has been developed based on a set of scientific and engineering principles including: material and energy balances, correlations describing the heat and mass transfer, and the thermo-physical properties of the working fluids. Additional instrumentations were installed in the chiller to make possible the calculation of heat and mass transfer coefficients in the various sections of the chiller at different conditions. Overall deviation between the measurements and the model simulation results are calculated based on the statistical analysis procedure to evaluate the model accuracy. At design condition, the overall deviation is about 5%. On the basis of the model analysis, the strategies to improve the chiller performance at the partial load conditions have been devised and the model has been validated to calculate chiller performance under various operating conditions.

**Key Words:** ***absorption chiller, model, measurement, performance, analysis***

## 1 INTRODUCTION

An absorption chiller is a machine, principally driven by heat (from direct firing of natural gas or other fuel or recovered heat from power generation or industrial processes, etc.), that produces chilled water for space and ventilation air-cooling. Generally only a minimal amount of mechanical energy or electric power is consumed in an absorption chiller for auxiliary devices (solution pump, water pumps, fans, controls, etc.). The BCT16 chiller has lowest rated capacity among commercially available double-effect absorption chillers. It is also available in models that are driven by natural gas and/or pressurized hot water at 160 °C.

An intensive testing and evaluation program has been carried out on a steam driven, double effect, parallel flow, 16 kW absorption chiller with its integral cooling tower. Figure 1 shows the absorption chiller installed on a platform adjacent to Carnegie Mellon's Intelligent Workplace, the IW. The chilled-water supply and return, steam supply, condensate return, power, and city water lines connect with the chiller at the bottom left. Figure 2 is a schematic flow diagram for the steam driven chiller recreated from the manufacturer's brochure for a commercial natural gas direct-fired chiller; this flow diagram shows all the heat and mass transfer components, pumps, and pipe fittings. It also indicates the design values for temperatures throughout the chiller. The components and parts indicated in Figure 2 are listed in Table 1.

Figure 1: BCT16 absorption chiller installed in the intelligent workplace (IW), Carnegie Mellon

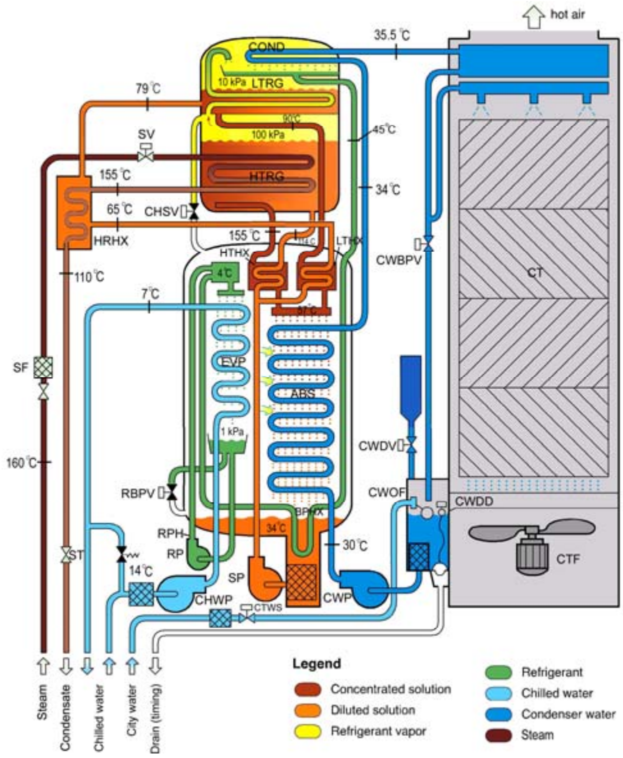


Figure 2: Schematic diagram of the absorption chiller

**Table 1: Component names and corresponding abbreviations**

| Abbreviation | Name | Abbreviation | Name |
|---|---|---|---|
| ABS | Absorber | EVP | Evaporator |
| BPHX | By-pass heat exchanger | HTRG | High-temperature regenerator |
| CHSV | Cooling/heating switch valve | HRHX | Heat recovery heat exchanger |
| CHWBPV | Chilled-water by-pass valve | HTHX | High-temperature heat exchanger |
| CHWP | Chilled-water pump | LTHX | Low-temperature heat exchanger |
| COND | Condenser | LTRG | Low-temperature regenerator |
| CT | Cooling tower | RBPSV | Refrigerant by-pass solenoid valve |
| CTOF | City-water overflow | RP | Refrigerant pump |
| CTWS | City-water switch | RPH | Refrigerant pump heater |
| CWBPV | Cooling-water by-pass valve | SF | Steam filter |
| CWDD | Cooling-water drain device | SP | Solution pump |
| CWDV | Cooling-water detergent valve | ST | Steam trap |
| CTF | Cooling-tower fan | SV | Steam valve |
| CWP | Cooling-water pump | | |

## 2 Test Program and Results

A system was set up to test the BCT16 absorption chiller and to evaluate its performance under a wide range of external and internal operating conditions. This test system, shown in Figure 3, comprises the following equipment in addition to the chiller:

- a steam supply system.
- a variable cooling load.
- an instrumentation, control, and data acquisition system.

The variable cooling load system can be adjusted independently and maintained constant during a test run. This load is provided by a shell-and-tube heat exchanger fed with hot water supply (HWS) to the shell from the building hot water grid. The flow of chilled water from the chiller outlet to the tubes of the load exchanger is controlled by a valve to achieve a desired flow set point. The flow of hot water to the exchanger is also controlled by a valve (BHWSV) to maintain a desired set point temperature for the chilled water at the inlet to the chiller.

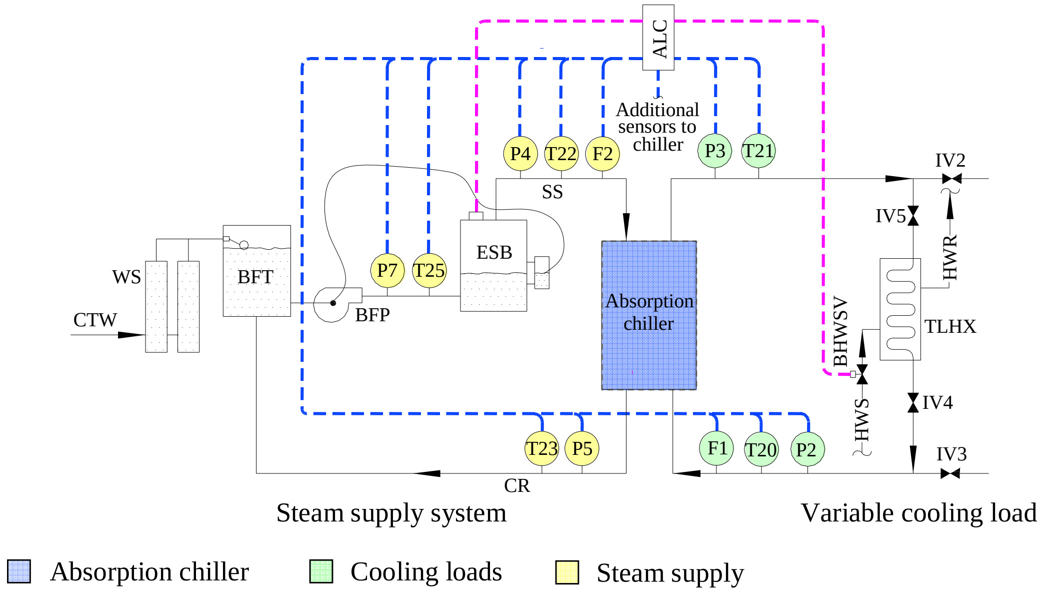


**Figure 3: Simplified flow diagram of the chiller test system**

A web based data acquisition and control system (ALC) was developed and installed to operate the chiller and its auxiliary equipment while storing and displaying the test measurement data. The chiller was tested at various operating conditions in accordance with a test program. On the basis of the test program, the effects of varied chilled water, cooling water, and steam input operating conditions on the chiller coefficient of performance and capacity were examined systematically. The chiller performance was calculated and presented on the basis of the measurement data gathered in the test program. The calculated chiller performance data under various load conditions checked and supplemented the performance data from manufacturer publications.

Figure 4 is the process and instrumentation diagram for the chiller. This figure illustrates chiller components, piping, and the measurement and control points. In Figure 4, the sensors from the manufacturer are indicated in green. The additional temperature sensors and flow meters installed to characterize the chiller performance are indicated in blue. The red lines indicate the control points of the chiller from the manufacturer, and the pink ones refer to the controls for the steam supply and cooling-load systems. The instruments and sensors installed in the chiller by its manufacturer indicate chiller operating conditions. All of these temperature, level, flow, and electric power measurements are listed in Table 2.

Eleven additional temperature sensors and a flow meter were installed in the chiller for this study to obtain further information on its operation, Table 2. The temperature sensors were mounted on the surface of the chiller vessel and piping. Serious consideration was given to installing of three pressure sensors to indicate pressure levels in the evaporator and in each of the two regenerators of the chiller. The chiller manufacturer advised against penetrating the chiller housing because of the possible introduction of air leakage or corrosion at the point of sensor installation. In Table 2, the sensors installed by the chiller manufacture use SI units, the addition temperature sensors and flow meters installed for chiller tests use IP units. Eventually, the computational model converts all IP Units into SI units for calculation.

A chiller test program was planned and executed. Each of the five operating conditions, identified above, was varied one at a time over a range of values, as indicated in Table 3. Within its range, each operating condition was tested at 5 to 10 values. The ranges for each of these five variables and their effects on chiller performance parameters are indicated in Table 3. Each test collected 20 to 200 data sets obtained at 2-minute intervals during steady-state operation of the chiller. A total of 38 tests were conducted over an estimated 220 hours of chiller operation. The results of all these tests in terms of the steam flow and chilled-water outlet temperature, the chiller load and the COP, is reported and discussed (Yin 2006).

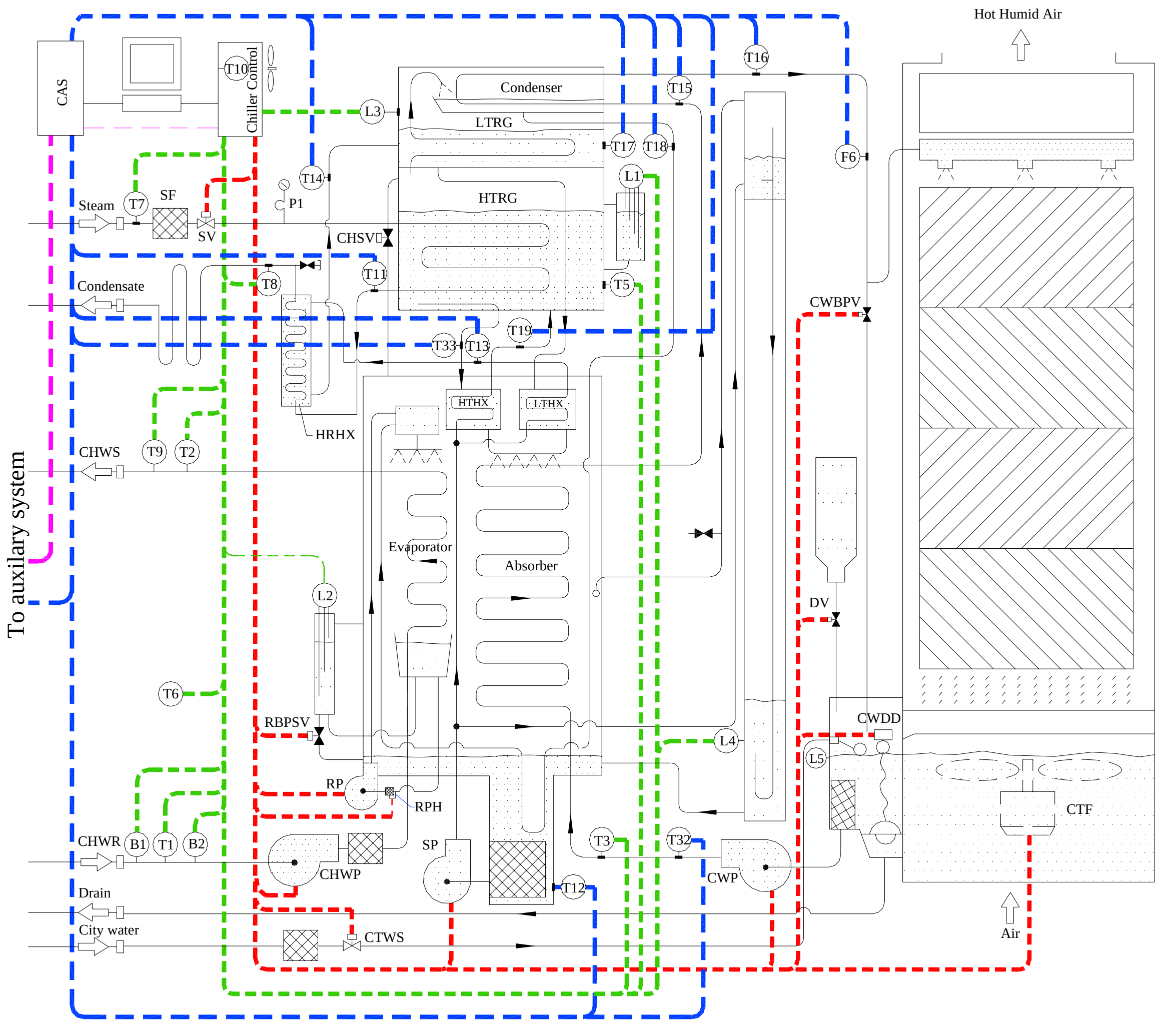


**Figure 4: PI&D diagram of the absorption chiller**

## 3 Chiller Performance Model

A comprehensive computational model was developed to further refine the understanding of the principles of the chiller, to analyze the experimental data from the test program, to assist in equipment design, and to evaluate the performance of various BCHP systems. This model is a set of equations consisting of: mass balances, energy balances, relations describing heat and mass transfer, and equations for the thermophysical properties of the working fluids. (Heold, Rdermacher, and Klein 1996) (Gommed and Grossman 1990) On the basis of the schematic flow diagram in Figure 2, a simplified flow diagram labeled with corresponding numbered state points was constructed as illustrated in Figure 5. Each state point is represented by its pressure, temperature, composition, and flow rate. The bold lines represent the water refrigerant (vapor/liquid); the other lines refer to the sorbent water-LiBr solutions. (Alefeld et al. 1994).

**Table 2: Instrumentation of the chiller test systems**

| | | Label | Sensor location | Medium | Range | Manufac. Accuracy | Onsite Calibr. |
|---|---|---|---|---|---|---|---|
| Absorption Chiller (manufacturer) | Temp. | **T1** | Chilled-water return | Water | (-15 °C) to 110 °C | ± 0.1% | |
| | | **T2** | Chilled-water supply | Water | (-15 °C) to 110 °C | ± 0.1% | |
| | | **T3** | Cooling-water supply | Water | (-15 °C) to 110 °C | ± 0.1% | |
| | | **T5** | High-temperature regenerator | Solution | (-15 °C) to 210 °C | ± 0.1% | |
| | | **T6** | Ambient | Air | (-15 °C) to 110 °C | ± 0.1% | |
| | | **T7** | Steam supply | Steam | (-15 °C) to 210 °C | ± 0.1% | |
| | | **T8** | Condensate return | Water | (-15 °C) to 210 °C | ± 0.1% | |
| | | **T9** | Chilled-water return 2 | Water | (-15 °C) to 110 °C | ± 0.1% | |
| | Level | **L1** | HTRG solution level probe | Solution | 4 pins | | |
| | | **L3** | LTRG upper-limit level probe | Solution | 1 pin | | |
| | | **L4** | Auto vacuum device level probe | Solution | 1 pin | | |
| | | **L5** | Cooling-water level probe | Water | 1 pin | | |
| | Flow | **B1** | Chilled-water flow detector | Water | on/off | | |
| | | **B2** | Chilled-water flow detector | Water | on/off | | |
| | Power | **D1** | Solution pump frequency, amps, and voltage | Electricity | | | |
| | | | | | | | |
| Absorption Chiller (ALC) | Temp. | **T11** | Condensate after HTRG | Surface | 0-400 °F | ± 0.1% | 0.5 °F |
| | | **T12** | Solution in Absorber | Surface | 0-400 °F | ± 0.1% | 0.5 °F |
| | | **T13** | Solution entering HRHX | Surface | 0-400 °F | ± 0.1% | 2 °F |
| | | **T14** | Solution leaving HRHX | Surface | 0-400 °F | ± 0.1% | 1.5 °F |
| | | **T15** | Cooling water after absorber | Surface | 0-400 °F | ± 0.1% | 1.5 °F |
| | | **T16** | Cooling water after condenser | Surface | 0-400 °F | ± 0.1% | 1.0 °F |
| | | **T17** | Low-temperature regenerator | Surface | 0-400 °F | ± 0.1% | 0.3 °F |
| | | **T18** | Refrigerant after condenser | Surface | 0-400 °F | ± 0.1% | 1.5 °F |
| | | **T19** | Refrigerant from evaporator | Surface | 0-400 °F | ± 0.1% | 2.0 °F |
| | | **T32** | Cooling water after cooling tower | Surface | 0-400 °F | ± 0.1% | 0.0 °F |
| | | **T33** | HTRG temperature | Surface | 0-400 °F | ± 0.1% | 1.5 °F |
| | Misc. | **F6** | Cooling-water flow | Water | 0 to 30 gpm | ± 1% | -15% |
| | | **E1** | Electric power of absorption chiller | Electricity | 0-2400 amps | ± 1% | 0.0% |
| Steam System | Temp. | **T22** | **Steam-supply temperature** | **Steam** | **(50 °F) to 250 °F** | ± **0.1%** | 0.0 °F |
| | | **T23** | **Condensate-return temperature** | **Water** | **(50 °F) to 250 °F** | ± **0.1%** | 0.0 °F |
| | | **T25** | Feed-water temperature | Water | (50 °F) to 250 °F | ± 0.1% | 0.0 °F |
| | Pres. | **P4** | Steam supply pressure | Steam | 0 to 40 gpm | ± 0.13% | |
| | | **P5** | Condensate return pressure | Water | 0 to 100 psi | ± 0.13% | |
| | | **P7** | Feed-water pressure | Water | 0 to 50 psi | ± 0.13% | |
| | Misc. | **F2** | **Steam flow** | **Steam** | **0 to 75 lb/h** | ± **0.5%** | **0-10%** |
| | | **E2** | Electric power of steam boiler | Electricity | 0-2400 amps | ± 1% | 0.0% |
| Cooling Load | Temp. | **T20** | **Chilled-water supply** | **Water** | **(-10 °F) to 110 °F** | ± **0.1%** | 0.6 °F |
| | | **T21** | **Chilled-water return** | **Water** | **(-10 °F) to 110 °F** | ± **0.1%** | -0.4 °F |
| | | **T31** | Ambient temperature | Air | (-58 °F) to122 °F | ± 0.1% | |
| | Pres. | **P2** | Chilled-water inlet | Water | 0 to 100 psi | ± 0.13% | |
| | | **P3** | Chilled-water outlet | Water | 0 to 50 psi | ± 0.13% | |
| | Flow | **F1** | **Chilled water** | **Water** | **0 to 20 gpm** | ± **1%** | **0%** |
| | | | | | | | |

**Table 3: Input and primary output of the test program**

| | Inputs | | | | | Primary Outputs | | Calculated performance | |
|---|---|---|---|---|---|---|---|---|---|
| | CHW return T | CHW flow | CW supply T | CW flow | Steam pressure | Steam Flow | CHW supply | COP | Cooling load |
| | $^oC$ | kg/s | $^oC$ | kg/s | kPa | kg/s | $^oC$ | | kW |
| Design condition | 13.9 | 0.5616 | 30.78 | 1.546 | 600 | 0.00727 | 7 | 1.03 | 16.63 |
| CHW return T | 8–14 | Design | Design | Design | Design | 0.00382–0.00771 | 6.25–6.9 | 0.95–1.03 | 9–18 |
| CHW flow | Design | 0.531–0.864 | Design | Design | Design | 0.00705–0.00771 | 6.42–8.97 | 0.93–1.02 | 16.56–17.96 |
| CW supply T | Design | Design | 27.5–36 | Design | Design | 0.00609–0.00764 | 6.13–9.26 | 1.11–0.91 | 19.22–13.29 |
| CW flow | Design | Design | Design | 0.784–1.547 | Design | 0.00618–0.00709 | 7.52–9 | 0.81–0.98 | 11.73–15.23 |
| Steam pressure | Design | Design | Design | Design | 360–700 | 0.00556–0.00748 | 6.34–10.27 | 0.65–0.99 | 8.41–17.47 |

The model for each chiller component In Figure 5 consists of equations representing mass balances for water and LiBr, the energy balance, the working fluids property relations, and the heat and mass transfer relations involving the state point conditions of the streams entering and leaving the component. The basic chiller model involves 416 variables and 409 nonlinear algebraic equations. Solving the model and determining values for all the chiller variables therefore requires specifying values for seven operating parameters. In this work, the specified operating parameters are: the chilled water inlet and outlet temperatures and flow, the cooling-water supply temperature and flow, the steam supply pressure and flow. Heat and mass transfer correlations have been integrated into the model so that it can evaluate the chiller performance not only at design conditions, but also at various off design conditions. (Chun et al. 1971) (Cosenza et al. 1990) (Dittus et al. 1930) (Vilet et al. 1982)

## 4 Model Based Data Analysis

The comprehensive model has been used to assess the accuracy of the experimental data from the test program. The discrepancies between the measurements and the model calculations were reduced by adjusting the model assumptions. The discrepancies between the measurements and the model solutions are introduced mainly by the following factors:

- inaccurate stream flow temperature measurements from sensors mounted on the external pipe surface
- fluctuating measurements of steam flow due to periodic feedwater addition to the boiler
- imprecise cooling-water flow measurements because of space limitations in mounting the flow sensor
- inaccurate assumptions regarding the quality of the refrigerant flow from various chiller components
- inaccurate values of heat transfer coefficients calculated from available correlations

The absorption cycle for each test has been plotted on a Dühring diagram based on the model calculations. In such a plot, many design parameters can be illustrated, such as the heat rejection temperatures, solution concentrations, equilibrium pressures, and pinch point of each heat transfer component. In Figure 6, the bold lines in the middle of the figure are the water-LiBr sorbent solution, and the bold dashed lines represent the refrigerant.

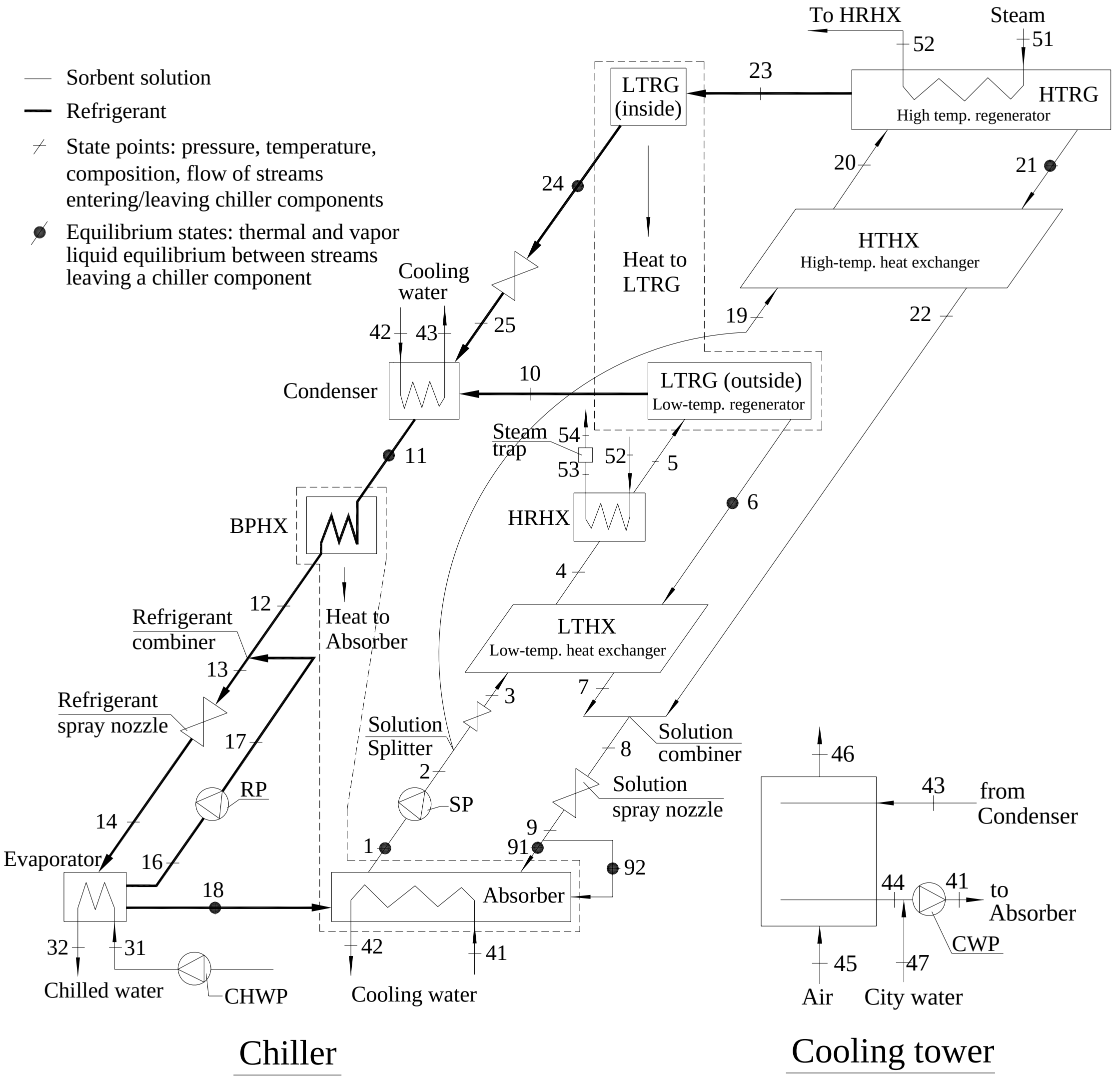


**Figure 5: Simplified flow diagram for chiller model**

## 5 Various Performance Curves

Figure 7 shows that the chiller COP calculated by the model is, on average, higher than that determined from measurement by 8%. The reason for the discrepancy is the calculation of the heat input. The model and the measurement share the same steam inlet pressure/temperature and the flow, but in the measurement the condensate from the chiller is assumed to be saturated water at atmospheric pressure. The model solution, however, shows that the condensate is partially vaporized when it leaves the chiller above an 82% design load. In the model, the heat input is defined by the summation of the heat transferred to the HTRG and the HRHX. The model, therefore, predicts lower quantity of heat transferred to the chiller than the measurements. Below 82% load conditions, the model predicts higher condensate return temperature than the measurements. Theoretically, the performance curve calculated by the model is a better representation of the chiller performance. The power consumption of the chiller is approximately 8% of the total energy supplied; the thermal COP is usually used to represent chiller performance.

The quantity of heat transferred in each component in the chiller is illustrated in Figure 8. The load in the 5 major heat transfer components is linearly related to the cooling load. The heat transferred on the 4 minor heat recovery exchangers, the HTHX, LTHX, HRHX, and BPHX, are relatively constant. Figure 9 shows the flow rates of the dilute sorbent solution from the absorber to the HTRG and LTRG at various load conditions. The dilute solution flow in the HTRG remains relatively constant. The sorbent solution flow rates to the LTRG decrease with the drop of cooling loads. This result is consistent with the chiller control principle that the variable frequency solution pump maintains the sorbent solution level in the HTRG.

In Figure 10, the refrigerant vaporization temperature in the evaporator at state point 18 is plotted. The refrigerant vaporization temperature is in equilibrium with the vapor pressure in the absorber. The refrigerant has a higher vaporization temperature, around 3.2 °C at design conditions; this temperature drops to 0.5 °C at 34% design load conditions. The result agrees with the observation that when the cooling load drops too low, ice may form in the evaporator. Ice formation affects chiller operation by blocking the spray nozzles.  This problem may be solved automatically when the chiller stops for a short while.

The vapor qualities of the chiller internal conditions at different state points are assumed in the model. The refrigerant vapor from the HTRG at state point 23 was initially assumed to be completely condensed in the LTRG, so only saturated water enters the condenser at state point 24. This assumption results in high estimated COP values because it is assumed that the LTRG recovers all latent heat of condensation. The values of vapor quality q24 have been adjusted as shown in Figure 11. The overall and weighted deviations of measured and calculated COP values are reduced by using these new q24 values. The chiller performance can be improved by appropriate measures for reducing the liquid carryover.

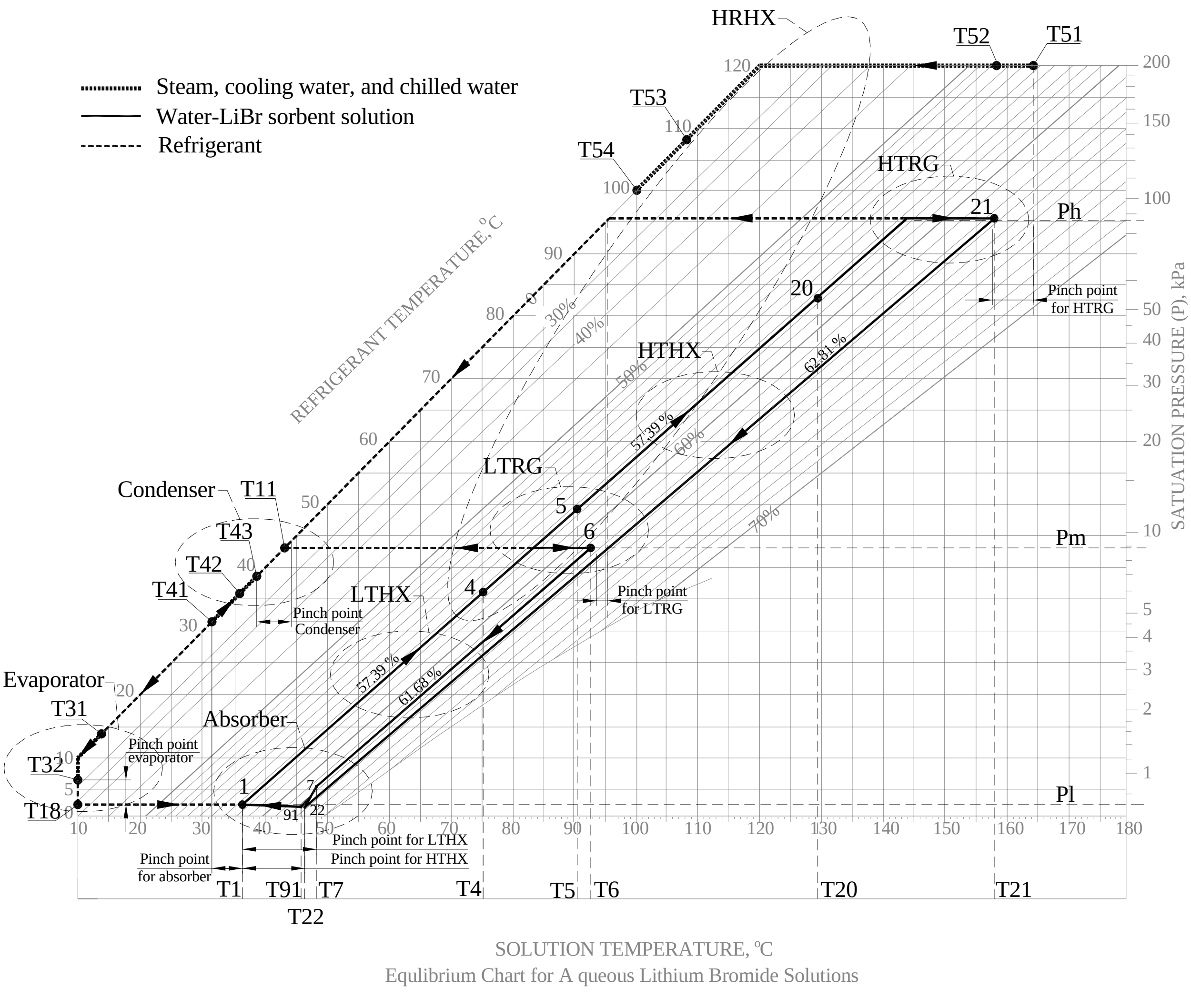


**Figure 6: Dűhring chart at design condition**

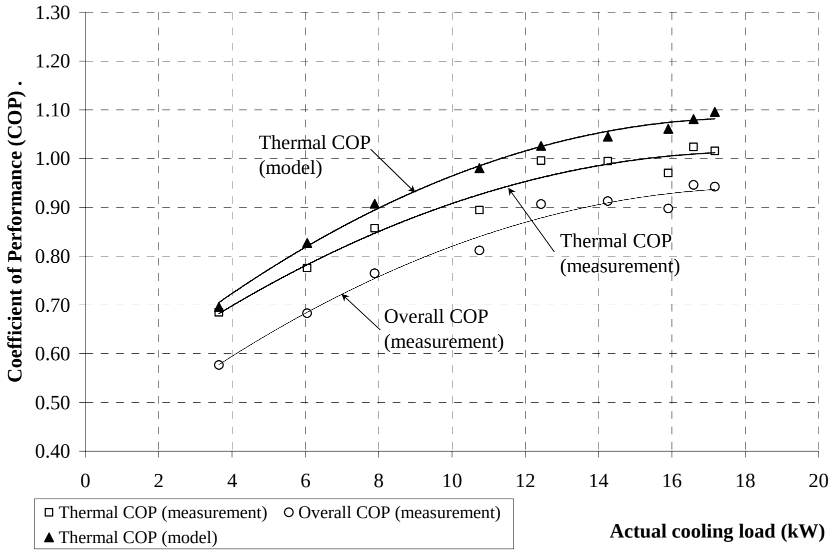


**Figure 7: Chiller performance curve under various load conditions**

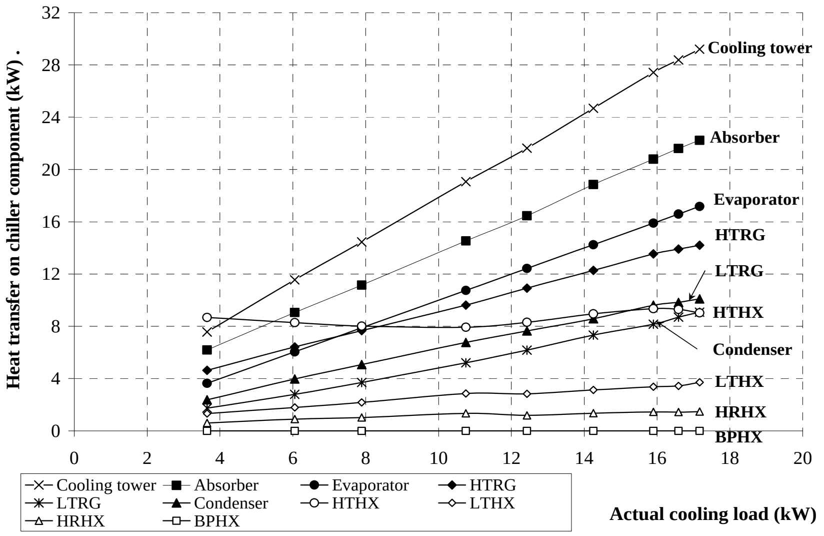


**Figure 8: Heat transfer load on each component under various load conditions**

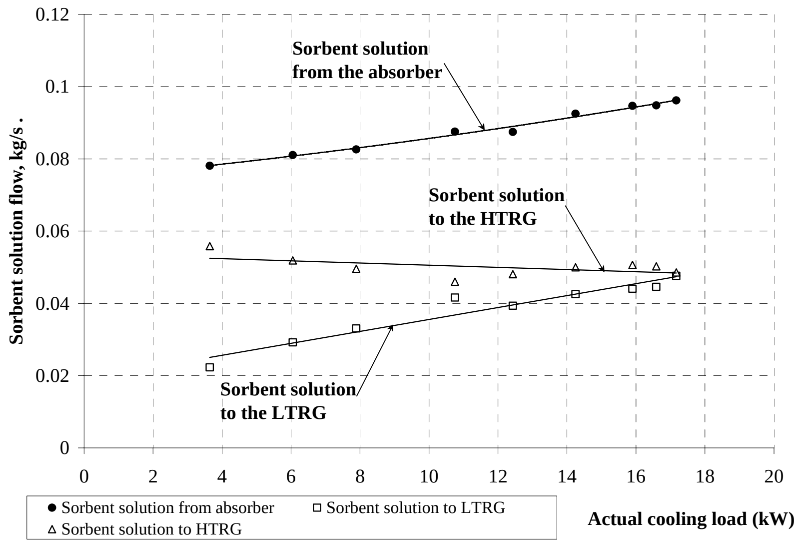


**Figure 9: Sorbent solution flow rate under various load conditions**

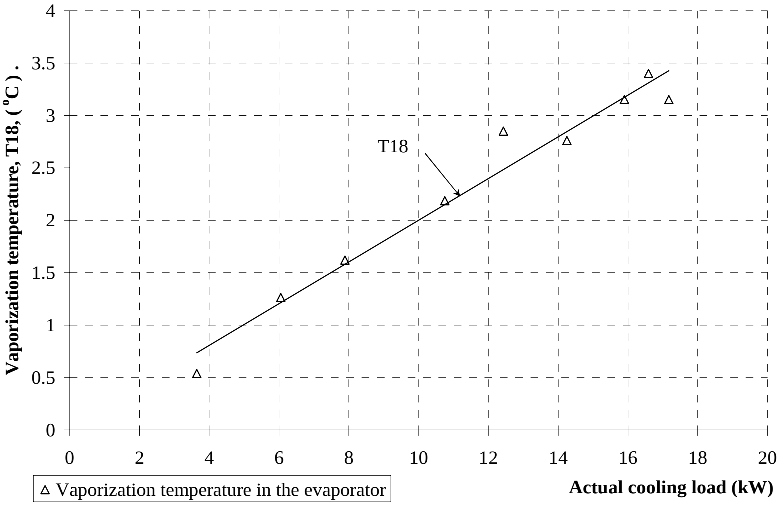


**Figure 10: Refrigerant vaporization temperature under various load conditions**

## 6 Heat Transfer Area Variations

The UA values of the 5 major heat transfer components are plotted in Figure 12. The model initially assumes that the contact area (As) of each heat transfer component remains constant. The model analysis, however, shows that the decrease in surface contact areas for the heat transfer components in the evaporator, and the LTRG under partial load conditions may partially contribute to the fast decrease of UA values. The variations of contact areas in the evaporator and the LTRG are due to the significant flow rate changes. Figure 13 shows the estimations of the area changes in the evaporator and the LTRG on the basis of the overall deviations between the measured values and the model solutions.

The surface area for the evaporator is also indicated in Figure 13. The surface contact areas decrease at partial load conditions by 30-50%. The reason for this change is the significant refrigerant flow decrease. The surface variations also exist in the LTRG because of the flow decrease from the design load condition to the partial load condition. Figure 9 indicates that the sorbent solution distributed to the LTRG drops from 0.048 kg/s at design load condition to 0.022 kg/s at 34% of design load condition. The chiller controls the solution levels in the HTRG but not in the LTRG. Under the lower load conditions, some of the tubes in the LTRG may be exposed to the refrigerant vapor. The surface contact areas of the HTRG, condenser, and absorber are not significantly affected by the load variations.

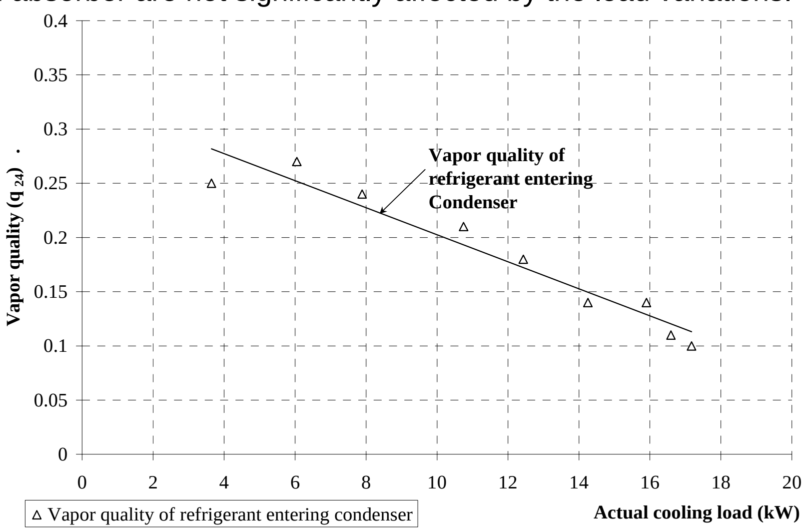


**Figure 11: Refrigerant vapor quality leaving the LTRG under various load conditions**

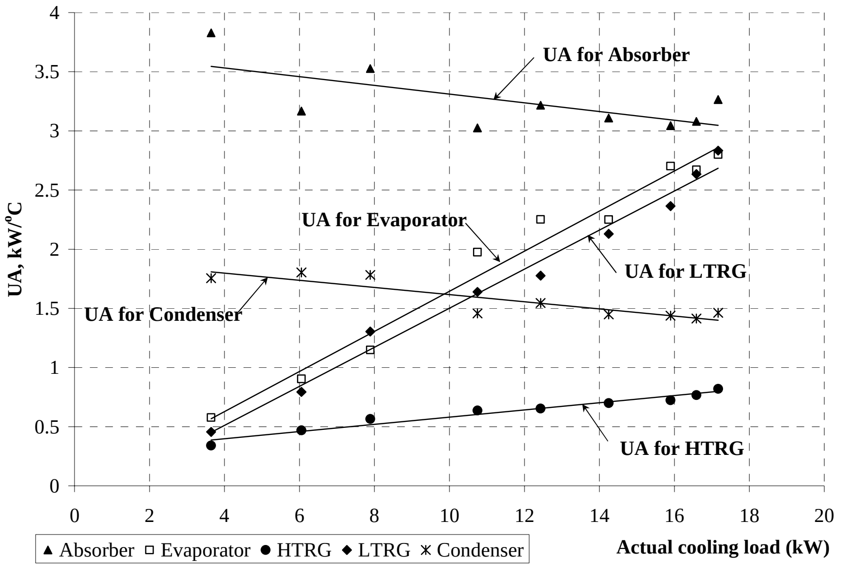


**Figure 12: UA changed for the 5 major components under various load conditions**

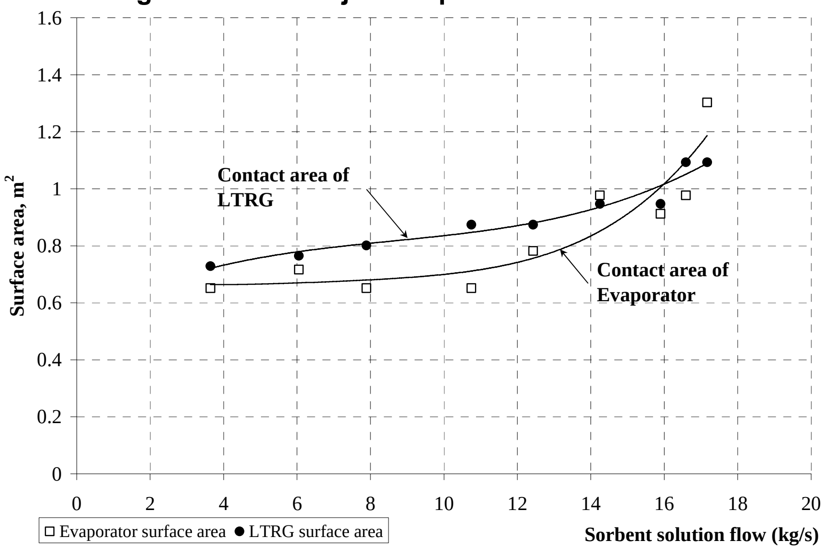


**Figure 13: Surface contact area changes under various load conditions**

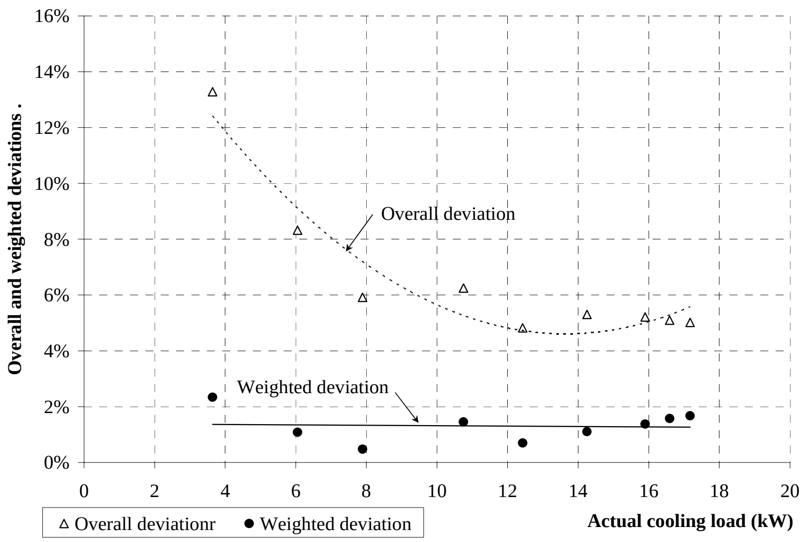


**Figure 14: Overall and weighted deviations under various load conditions**

## 7 Deviation Variations

The statistical analysis procedure is used to evaluate the deviations between the model calculations and the test measurements. The overall deviations and the weighted deviations of the measurements and the model solutions are plotted in Figure 14. The overall deviations are below 6% when the cooling loads are above 60% of the design condition. When the load drops below 60%, the overall deviations increase fast to 13% at 34% of design load condition. The dramatic increase of overall deviation is due to the inaccuracy of steam flow measurements and the relative increasing discrepancy of condensate return temperature between the measured values and the model solutions. By using the weights in the model, the overall deviation between the model solutions and the measurements is less affected by the uncertainties of the measurements. The weighted deviation for all operation condition is around 2%.Only the results of the cooling-load variation tests have been presented in this section. The analyses of other test data are presented by (Yin 2006) regarding the effects on the COP, capacity, and chilled water supply temperature of chilled-water supply temperature, chilled-water flow rate, cooling-water supply temperature, cooling-water supply flow rate, steam supply temperature.

## 8 Summary

This study develops methods for the effective design and evaluation of an absorption chiller for micro-BCHP systems that reduce energy consumption, decrease operational costs, and improve environmental benefits in residential and light commercial buildings. The field of computational support for building an energy system is extensive, and this study has illustrated significant concepts in designing, analyzing, and modeling of absorption chiller systems and of analyzing extensive test data sets with the support of a detailed model.

## 9 REFERENCES

Alefeld, G., Radermacher, R., 1994, Heat Conversion Systems, CRC Press Inc., Boca Raton, FL

Chun, K.R., and Seban, R. A., 1971, “Heat Transfer to Evaporating Liquid Films,” Journal of Heat Transfer, 91c, page 391-396"

Cosenza, F. Vliet, G. C., 1990. “Absorption in Falling Water-LiBr Films on Horizontal Tubes,” ASHRAE Transactions 96910, pp693-701

Dittus, F. W., and Boelter, L. M. K. 1930, “University California Berkeley Pub. Eng., Vol. 2, p.443”

Herold, K. E., Radermacher R., Klein S. A., 1996, Absorption Chillers and Heat Pumps, CPC Press, Inc., Boca Raton, FL.

Holman, J. P. 1997, “Heat transfer”, 8th edition, the McGraw-Hill Companies, Inc.

Hottel, H. C., 1967, “Chapter 6, Gas Emissivities and Absorptivities,” Radiative Transfer, pp. 234, McGraw-HIill

Vliet, G. C., Lawson, M. B., and Lithgow, R. A., 1982, “Water-Lithium Bromide Two-stage Absorption Cooling Cycle Analysis, ” ASHRAE Transaction, 88, Part1, 811-823

Yin, H. 2006, "An Absorption Chiller in a Micro BCHP Application: Model Based Design and Performance Analysis." PhD Thesis, Carnegie Mellon University, School of Architecture, 6 September